*J. Bangladesh Acad. Sci., Vol. 44, No. 1, 59-68, 2020*
*DOI: https://doi.org/10.3329/jbas.v44i1.48564*

# IDENTIFICATION OF MULTIPLE RARE EARTHS AND OTHER ASSOCIATED ELEMENTS IN ZIRCON BY LASER-INDUCED BREAKDOWN SPECTROSCOPY

A. F. M. Y. HAIDER[1,2] AND ZULFIQAR HASAN KHAN[1*]
[1]*Department of Physics, University of Dhaka, Dhaka 1000*

## ABSTRACT

Laser-induced breakdown spectroscopy (LIBS), which is a powerful technique for the detection of minor and trace elements in a sample, has been used to analyze the enriched zircon mineral collected from the beach sands of southern Bangladesh. In addition to zirconium, a large number of rare earth elements viz. cerium, lanthanum, praseodymium, neodymium, ytterbium, gadolinium, dysprosium, erbium, samarium, europium, holmium and yttrium and other associated elements like hafnium, niobium, tantalum, magnesium, calcium, sodium, titanium and iron along with non-metals like phosphorus and silicon were detected in the enriched zircon samples by the LIBS technique. To the best of our knowledge, this is the first time that multiple rare earth elements have been identified in natural zircon by LIBS.

**Keywords:** Laser-induced Breakdown Spectroscopy, Zircon, Rare Earth Element

## INTRODUCTION

Laser-induced breakdown spectroscopy (LIBS) (Cremers *et al.* 2006, Singh *et al.* 2006, Miziolek *et al.* 2006) is a versatile technique for the elemental analysis, where a high-power pulsed laser beam is focused on the sample to generate a high-temperature transient plasma. The emitted light from the plasma contains a spectral signature of elements present in the sample. This technique has been applied in different fields, such as in industry (Aragon *et al.* 1993, Gruber *et al*. 2001), environmental monitoring (Arca *et al.* 1997), mars exploration (Colao *et al.* 2004), coal, and mineral analysis (McMillan *et al.* 2007, McMillan *et al.* 2006, Haider *et al.* 2011).

India, China, Australia, Brazil, and Bangladesh have sandy beaches containing heavy minerals such as magnetite, monazite, ilmenite, rutile, zircon, and other minor minerals (Gupta *et al.* 2005). Rutile, zircon, and monazite are valuable minerals because of their commercial value and the rare earth elemental (REE) contents.

For detection and quantification of REEs, different sophisticated analytical techniques are typically used, such as inductively coupled plasma mass spectrometry (ICP-MS), inductively coupled plasma optical emission spectrometry (ICP-OES), X-ray photoelectron spectroscopy (XPS) and instrumental neutron activation analysis (INAA). However, both ICP-MS and ICP-OES require time-consuming sample preparation. INAA technique requires access to a nuclear reactor, and long irradiation time is needed for direct analysis of REE in a solid sample (Balaram 2019). Besides, XRF demonstrates low sensitivity for REE detection (De Vito *et al.* 2000). Because of the higher detection limit, separation and preconcentration processes are sometimes needed to be accompanied by XRF to improve the sensitivity for REE detection (De Vito *et al.* 2000). The use of LIBS for REE detection is advantageous because of the requirement of little to no sample preparation and rapid, in situ/real-time detection of REE with adequate sensitivity (Balaram 2019).

*Corresponding author: <zulfiqarshuvo@du.ac.bd>.
[2]Department of Mathematics and Natural Sciences, BRAC University, Dhaka-1212, Bangladesh

Detection of REE by LIBS has been reported by several groups using lab-prepared samples of lanthanide compounds (Alamelu *et al.* 2008, Yun *et al.* 2001). On the other hand, Abedin *et al.* (Abedin *et al.* 2011) and Haider *et al.* (Haider *et al.* 2011) reported the detection of several REEs in raw monazite sands and coal ash, respectively, by LIBS technique. However, there is no report on the detection of REEs in zircon mineral by LIBS technique. Since natural mineral zircon contains other elements (such as silicon, titanium, and iron), having their strong emission lines which may interfere with that of REEs, the detection and identification of REEs in this mineral is not a trivial job.

Beach Sand Minerals Exploitation Centre (BSMEC) of Bangladesh Atomic Energy Commission (BAEC) has been exploring and exploiting valuable minerals from the coastal areas of Bangladesh for over three decades. The center has separated eight prominent heavy minerals of economic importance: ilmenite, magnetite, zircon, rutile, garnet, monazite, leucoxene, and kyanite in the beach sands of Bangladesh (enrichments of these heavy minerals are as high as 90%). The estimated reserve of these eight heavy minerals is about 1.76 million tons in the beach sands of Bangladesh (Akon 2019, Chowdhury *et al.* 2014).

Zircon is a mineral belonging to the group of nesosilicates. Its chemical name is zirconium silicate ($ZrSiO_4$). When REEs substitutes some zircon atoms, the standard empirical formula for zircon becomes (Zr, Ln) $SiO_4$, where Ln represents lanthanides (Dostal 2017). The crystal structure of zircon is tetragonal. Zircon is non-magnetic and has poor electrical conductivity. An essential use of zirconium is for nuclear reactor fuel cladding (in the form of zircaloys) because of its low neutron-capture cross-section and resistance to corrosion (Krishnan *et al.* 1981). Resistance to corrosion and erosion makes the zircon products ideal for the chemical industry and desalination plants (Bermúdez *et al.* 2005). High-temperature parts, such as combustors, blades, and vanes in modern jet engines and stationary gas turbines, are protected against thermal damage by thin ceramic layers composed of a mixture of zirconium and yttrium oxide (Peters *et al.* 2001).

REEs possess unique spectroscopic and magnetic properties. Rechargeable batteries, mobile phones, plasma televisions, disk drives, and catalytic converters all use one or the other unique properties of REEs. The most crucial application of rare earth metals is in the world's production of the strongest permanent magnets made of cobalt and samarium (Haque *et al.* 2014).

In this paper, we analyzed the LIBS spectrum of enriched zircon mineral extracted from beach sands of southern Bangladesh by using the LIBS technique and identified many spectral lines of REEs in addition to some other metallic and non-metallic elements.

## EXPERIMENTAL SETUP

The schematic diagram of the experimental LIBS set up is shown in Fig. 1. A Q-switched Nd:YAG laser (Spectra-Physics LAB-170-10) having an output at the fundamental wavelength of 1064 nm with a pulse duration of 8 ns and repetition rate of 10 Hz and maximum pulse energy of 850 mJ was the excitation laser. It was also equipped with harmonic generators capable of generating up to fourth harmonics of the fundamental employing KDP crystals. The actual pulse energy used was 40 mJ. The beam has a Gaussian profile in the far-field with a beam divergence of less than 0.5 mrad. The

experiments were performed in air (Abedin *et al.* 2011, Haider *et al.* 2012, Haider *et al.* 2011).

The output of the Nd: YAG laser at the fundamental was focused on the sample by a convex lens of 100 mm focal length to produce intense, transient, and weakly ionized plasma. The spot size at the sample position was about 200 µm, and the peak power density for 40 mJ pulses was 16 GW/cm$^2$. The plasma was generated at the repetition rate of the laser (10Hz).

The light emitted from the plasma was focused by a fused quartz lens (f=50 mm) and collected by a 3 m long multi-mode silica fibre. The output end of the optical fiber was placed at the entrance slit of a 750 mm focal length computerized Czerny-Turner spectrograph (Acton Model SP-2758). The spectrograph is equipped with three ruled gratings: 2400, 600, and 300 grooves/mm blazed at 240, 500, and

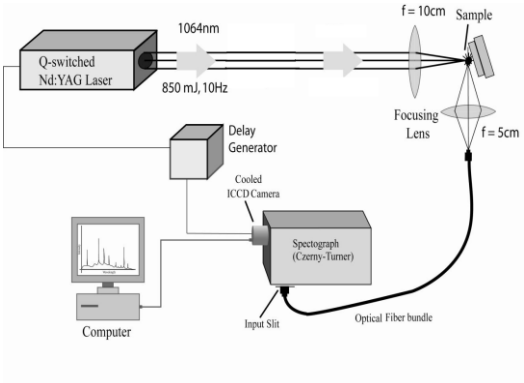


**Fig. 1.** Schematic diagram of the LIBS experimental setup.

300 nm, respectively, which are interchangeable under computer control, providing high-and low-resolution spectra in the wavelength range of 190–880 nm. If 600 grooves/mm grating is used, a spectrum of about 38 nm in width can be captured without moving the grating, and for the 2400 grooves/mm grating, it is about 9 nm. However, these widths are insufficient to cover all the wavelengths of the emission spectrum from the sample. Hence, the grating was stepped under computer control, and a separate spectrum was acquired for each grating position to cover a wider spectral range (Abedin *et al.* 2011, Haider *et al*. 2012, Haider *et al.* 2011).

An intensified and gated CCD camera (Princeton PI-MAX with Unigen II coating and programmable delay generator) was coupled to the spectrograph's output end. The ICCD camera used has 1024X1024 pixels and was cooled to -20$^0$ C by using Peltier cooling to reduce noise. The ICCD camera was electrically triggered by the Nd:YAG laser pulse after a software-controlled, adjustable time delay. In this way, the intense background radiation initially created by the high-temperature plasma was significantly eliminated, and the atomic/ionic emission lines of the elements were more clearly observed. In the present experiments, a delay time $t_d$ of 1.5 µs and a gate width $t_w$ of 50 µs were selected for the optimum signal. Usually, spectra from several laser shots (about 40–80) were acquired and averaged to increase the signal-to-noise ratio. Samples were manually moved between exposures to prevent crater formation and to avoid other deleterious effects. The spectrum, captured by the ICCD camera, was transferred to the personal computer by USB cable. A software (Win Spec/32) provided by the manufacturer was used to control all the functions of the gated ICCD camera and the Acton spectrograph (Abedin *et al.* 2011, Haider *et al.* 2012, Haider *et al.* 2011).

## SAMPLE PROCESSING

The sand collected from the beach was washed, dried, and panned in attempts to separate the lighter sands from the heavier ones. The sample was then passed through the magnetic separator, which separates the non-magnetic heavy minerals (zircon and rutile) from magnetic heavy minerals (Ilmenite and Garnet). Both magnetic

and non-magnetic heavy minerals were then passed through the separator, which separates conducting from non-conducting components. Of the non-magnetic parts, the non-conducting part was zircon.

Nevertheless, even after this physical separation of zircon, it contains other constituents like rutile (non-magnetic and conducting part), ilmenite (magnetic and conducting part) (Abedin *et al.* 2011). This physical separation of zircon was performed by BSMEC of BAEC. The enriched zircon mineral collected from BSMEC of BAEC was ground and passed through a 75-micron sieve. The purpose of grinding the zircon to powder form, subsequent sieving, and thorough mixing was to make the distribution of all the elements homogeneous throughout the sample volume. Therefore, matrix effect of the sample is eliminated or at least reduced to a minimum in the subsequent LIBS experiments. Finally, small pellets of zircon were prepared by using a hand press with sufficient pressure (~ 80 bars). About ten pellets were made and subjected to LIBS experiments, as described above (Haider and Khan 2012).

## RESULTS

The acquired LIBS spectra of zircon collected from the Beach Sand Mineral Exploitation Center, Cox's Bazar, Bangladesh, are shown in Fig. 2(a)-2(f) for some selected spectral regions. About 40-80 shots of the laser were averaged to acquire each spectrum. The average plasma temperature during the observation time window, estimated by the standard Boltzmann plot method (Cremers *et al.* 2006), was in the range of 9,000-11,000 K. The observed line peaks in the spectra were compared with the online NIST database available from the US National Institute of Standards and Technology (Anonymous 2019). Identified lines are shown in Fig. 2(a)-2(f). A large number of strong emission lines of titanium and iron were detected, which sometimes caused severe interference with the expected emission lines of REEs. An REE was considered being detected in our experiments only when at least five of its non-interfered lines were unambiguously identified. The identified REEs with their ionic states, the observed values of the wavelengths of the detected emission lines and the total number of unambiguously identified lines are shown in Table 1 for the enriched zircon mineral extracted from the beach sand. Table 2 shows the lines of both metallic and non-metallic elements in enriched zircon sand, co-existing with the REEs. Only non-interfered, unambiguously identified lines are shown. A significant number of transition metal elements were detected, whose origin will be explained later. Besides, non-metals like silicon and phosphorus were identified in the sample.

## DISCUSSION

In the above experiments, a large number of elements were simultaneously detected in the enriched zircon mineral separated from beach sand at BSMEC. Among these elements, the most interesting elements were the REEs such as cerium, lanthanum, neodymium, yttrium, ytterbium, gadolinium, dysprosium, erbium, samarium, europium, holmium (Table 1). All these REEs except holmium, were previously obtained in the analysis of monazite performed by our group using the same experimental setup (Abedin *et al.* 2011).

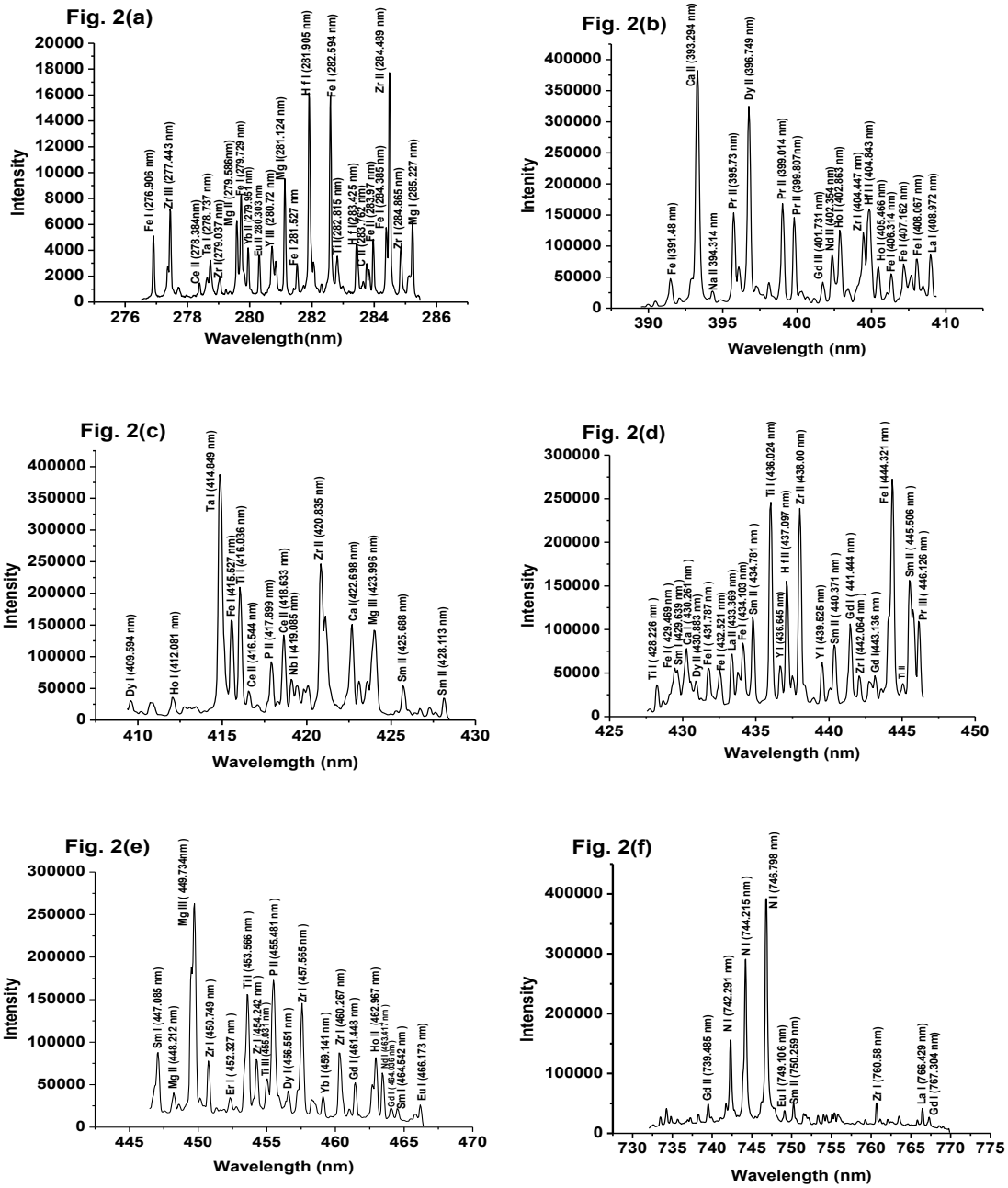


**Fig. 2 (a)-(f).** The LIBS spectra for zircon at different spectral regions. The major identified lines are shown.

Haider *et al*. (Haider *et al*. 2011) detected a lesser number of REEs, viz., Nd, Yb, Ce, Sm, and Gd in their coal ash samples using the same LIBS set up. Depending on the origin of the rocks from which they are formed, the zircon around the world shows some significant variations in their rare earth compositions (Gupta *et al.* 2005). Bangladesh Atomic Energy Commission found $ZrO_2$, $SiO_2$, $Fe_2O_3$, $TiO_2$, S, and P in zircon of southern Bangladesh by typical chemical analysis (Akon 2019). The REEs were probably present in minor or trace amounts and had hitherto remained undetected. Because of the relatively high sensitivity of the present LIBS set up (typically of the order of parts per million), they were detected in the present experiments.

**Table 1.** Emission lines of identified rare earth elements in zircon.

| **Elements identified** | **Wavelengths (nm) of Major Identified Lines (with ionic states )** | **Total no of identified lines** |
|---|---|---|
| Cerium (Ce) | 278.384(II),293.159(III),5.495(II),305.739(III),308.556(III),310.674(III),311.107(II),322.868(III)349.772(III),351.46(III), 362.408(II),383.658(II),416.544(II), 418.633(II), 650.723(II),720.242(I) | 16 |
| Lanthanum (La) | 338.045(II),375.901(II), 408.972(I), 433.369(II), 442.798(II), 466.277(II), 495.029(I),499.183(II),504.668(I),766.429(I) | 15 |
| Neodymium (Nd) | 352.747(II),382.3(II), 386.374(II), 402.354(II),463.417(I),471.97(I),486.715(I), 510.57(II), 520.056(II),557.73(I),562.09(I) | 12 |
| Yttrium (Y) | 280.72(III), 360.081(II), 436.645(I),439.525(I),467.517(I),475.35(I),483.96(I), | 10 |
| Ytterbium (Yb) | 251.638(II), 274.961(III),279.951(II), 302.946(III),313.886(III),340.373(II), 459.141(I),666.834(I) | 12 |
| Gadolinium (Gd) | 260.989(III),283.438(III),291.856(III),295.575(III),302.805(II),308.224(II),336.284(II), 340.824(II),350.555(II),354.955(II)348.124(II),365.528(II), 366.266(II), 367.457(I), 369.781(II), 371.935(II),379.639(II),384.28(II),401.731(III), 441.444(I),443.136(I), 461.448(I),464.036(I),739.485(II),767.304(I) | 29 |
| Dysprosium (Dy) | 340.824(II),345.473(II),353.537(II),354.233(II),355.189(II),357.697(II), 367.91(I),396.749(II),409.594(I),430.883(II),456.551(I), 512.03(I),820.162(II) | 18 |
| Erbium (Er) | 291.067(II),296.454(II), 326.473(II), 336.396(II), 336.809(II), 349.959(II),381.734(III,)452.327(I) | 11 |
| Samarium (Sm) | 325.034(II),332.154(II), 334.065(II),367.116(II),373.125(II),388.184(II),388.58(II),425.688(II),428.113(II), 429.639(I), 434.781(II), 440.371(II), 445.506(II), 447.085(I), 464.542(I), 488.457(I), 750.259(II) | 21 |
| Europium (Eu) | 237.519(III),261.939(I),274.073(II),280.303(II),287.62(II),292.501(II),301.858(III),333.462(I) 466.173(I),602.926(I),664.562(II), 749.106(I) | 15 |
| Holmium (Ho) | 256.788(II), 289.566(II),343.246(II), 389.088(I),402.863(I),405.466(I),412.081(I),462.967(II) ,760.58(I) | 9 |
| Praseodymium (Pr) | 300.819(III),387.788(II),395.73(II),399.014(II), 399.807(II),445.054(III),446.126(III),657.85(I) | 13 |

**Table 2.** Other detected elements in zircon.

| **Elements identified** | **Wavelengths (nm) of Major Identified lines (with ionic states)** | **Total no of identified lines** |
|---|---|---|
| Zirconium (Zr) | 264.388(III),266.45(III),268.225(III),277.443(III),279.037(I),284.489(II),284.865(I),294.902(II),302.05(II),303.087(II),310.674(II),313.362(II),323.426(I),339.216(II),343.832(II),349.611(II),351.955(I),352.586(II),354.77(I),355.656(II),404.447(I),420.835(II),438(II), 442.064(I),450.749(I),454.242(I), 457.565(I), 460.267(I),473.266(I),535.07(II) | 102 |
| Hafnium (Hf) | 264.165(II),281.905(I), 283.425(I),291.636(I),306.483(II),307.303(I),310.929(II),341.924(I), 353.698(I),404.843(II),437.097(II),631.251(I) | 14 |
| Niobium (Nb) | 210.958(II),259.39(III),323.654(II), 351.038(II), 379.186(I),419.085(I),481.654(I), 667.776(I) | 12 |
| Tantalum (Ta) | 238.728(II),264.756(I),265.676(I),271.443(I),275.9(I),278.737(I),331.146(I),414.849(I),468.532(I) | 11 |
| Magnesium (Mg) | 279.586(II),281.124(I),285.227(I),290.55(III),293.661(II),309.297(I), 353.895(II), 423.996(III), 448.212(II),449.734(III) | 13 |
| Calcium (Ca) | 315.925(II), 317.971(II), 373.749(II), 393.294(II),422.698(I),430.261(I),527.063(I),616.27(I),637.083(III) | 11 |
| Sodium (Na) | 330.258(I),336.946(II), 394.314(II), 589.048(I),589.661(I),646.236(II) | 10 |
| Silicon (Si) | 220.784(I), 288.192(I) | 5 |
| Phosphorus (P) | 417.899(II), 455.481(II), 519.159(II),547.88(I) | 6 |
| Titanium (Ti) | 282.815(I),331.007(I),332.96(II),334.203(I),334.944(II),335.457(I),336.133(II),363.6(I),376.694(I),416.036(I),428.226(I),436.024(I) ,453.566(I),455.031(III), 482.497(III) | 26 |
| Iron (Fe) | 246.416(II), 259.959(II), 262.084(II), 276.906(I),279.729(I),281.527(I),282.594(I),283.97(II),284.385(I),287.282(I),297.331(I),300.074(I),316.625(I),337.084(I),346.998(I),352.091(I),353.006(I), 374.598(I), 391.48(I), 406.314(I),407.162(I),408.067(I),410.837(I),415.527(I),425.744(I),429.469(I),431.787(I),432.521(I), 434.103(I),444.321(I),470.336(I),481.035(I),493.457(I),501.539(I),517.363(I),552.919(I), 559.519(I),615.826(I),625.69(I) | 58 |

Table 2 shows other elements detected in the zircon sample. Metallic elements such as zirconium, hafnium, niobium, tantalum, magnesium, calcium, sodium, titanium, and iron were also detected along with non-metals like phosphorus and silicon. In zircon, the high number of lines of zirconium and silicon are natural because zircon mainly comprises zirconium silicate ($ZrSiO_4$). Most of these transition metals and some other elements (e.g., titanium and magnesium) were earlier detected in the beach sands collected from the same geographical area using a non-gated, non-intensified, and relatively low sensitive LIBS system by our research group (Haider *et al.* 2010). In the present experiments, the highly sensitive, gated and intensified, ICCD system probably enabled us to detect many trace elements present in the sample.

The identified elements titanium and iron in our experiments have originated from rutile (TiO), magnetite ($Fe_2O_3$), and ilmenite ($FeTiO_3$) that may be present with zircon as the separation of the minerals by the physical method was not hundred percent (Abedin *et al.* 2011). Garnet contains appreciable quantities of calcium, magnesium and manganese (Tasneem *et al.* 2019), accounting for the presence of these lines in our experiments. Spectral lines of niobium and tantalum may have originated from the presence of a small amount of columbite, which is sometimes observed in Indian placer deposits (Abedin *et al.* 2011, Gupta *et al.* 2005). Zircon in silicate form melts with high field strength incompatible elements like hafnium (Schulz *et al.* 2018) that is the cause of the presence of hafnium lines in our sample.

## CONCLUSION

We have simultaneously detected several REEs such as cerium, lanthanum, praseodymium, neodymium, ytterbium, gadolinium, dysprosium, erbium, samarium, europium, holmium and yttrium in addition to other associated elements in enriched zircon minerals separated from beach sands of Bangladesh by the LIBS technique. In the present research, amongst the seventeen REEs, twelve were detected in our zircon sample. To the best of our knowledge, this is the first time that REEs have been identified in naturally occurring zircon mineral by LIBS technique. The standard addition method may be employed to determine the relative abundances of these REEs in the zircon sample collected from the beach sands. A commercially viable extraction of these REEs could be a profitable project for Bangladesh.

## ACKNOWLEDGEMENT

We acknowledge the useful discussion on the manuscript with Associate Professor Kazi M. Abedin of the physics department of the Sutan Qaboos University, Muscat, Oman. We also thank BSMEC of BAEC, Bangladesh for providing us with the Zircon sample.

## REFERENCES

Abedin, K., A. F. M. Y. Haider, M. Rony, and Z. Khan. 2011. Identification of multiple rare earths and associated elements in raw monazite sands by laser-induced breakdown spectroscopy. *Opt. Laser Technol.* **43**(1): 45-49.

Akon, E. 2019. Mineralogy, geochemistry and economic potentialities of heavy mineral sand resources of Bangladesh. *J. Nepal Geol. Soc.* **59:** 1-8.

Alamelu, D., A. Sarkar, and S. Aggarwal. 2008. Laser-induced breakdown spectroscopy for simultaneous determination of Sm, Eu and Gd in aqueous solution. *Talanta* **77**(1): 256-*261*.

Anonymous. 2019. *NIST Atomic Spectra Database Lines Form.* Available from https://physics.nist.gov/PhysRefData/ASD/lines_form.html.

Aragon, C., J. Aguilera, and J. Campos. 1993. Determination of carbon content in molten steel using laser-induced breakdown spectroscopy. *Appl. Spectrosc.* **47**(5): 606-608.

Arca, G., A. Ciucci, V. Palleschi, S. Rastelli, and E. Tognoni. 1997. Trace element analysis in water by the laser-induced breakdown spectroscopy technique. *Appl. Spectrosc.* **51**(8): 1102-1105.

Balaram, V. 2019. Rare earth elements: A review of applications, occurrence, exploration, analysis, recycling, and environmental impact. *Geosci. Front.* **10**(4): 1285-1303.

Bermúdez, M.-D., F. J. Carrión, G. Martínez-Nicolás, and R. López. 2005. Erosion–corrosion of stainless steels, titanium, tantalum and zirconium. *Wear* **258**(1-4): 693-700.

Chowdhury, M., and M. Sarker. 2014. Delineation of the Surface Pattern of Heavy Mineral Deposit of Tulatoli Paleo Dune Within Teknaf Beach Strip of Cox's Bazar District with Radiometric Survey.*Nucl. Sci. Appl. (Dhaka)* **23**(1-2): 33-36.

Colao, F., R. Fantoni, V. Lazic, A. Paolini, F. Fabbri, G. Ori, L. Marinangeli, and A. Baliva. 2004. Investigation of LIBS feasibility for in situ planetary exploration: an analysis on Martian rock analogues. *Planet. Space. Sci.* **52**(1-3): 117-123.

Cremers, D. A., and R. J. Radziemski. 2006. Handbook of Laser-Induced Breakdown Spectroscopy. U. K.: John Wiley & Sons.

De Vito, I. E., R. A. Olsina, and A. N. Masi. 2000. Enrichment method for trace amounts of rare earth elements using chemofiltration and XRF determination. *Fresenius J. Anal. Chem.* **368**(4): 392-396.

Dostal, J. 2017. Rare earth element deposits of alkaline igneous rocks. *Resources***6** (3): 34.

Gruber, J., J. Heitz, H. Strasser, D. Bäuerle, and N. Ramaseder. 2001. Rapid in-situ analysis of liquid steel by laser-induced breakdown spectroscopy. *Spectrochim. Acta Part B: At. Spectrosc.* **56**(6): 685-693.

Gupta, C. K., and N. Krishnamurthy. 2005. Extractive Metallurgy of Rare Earths: CRC Press.

Haider, A. F. M. Y., and Z. Khan. 2012. Determination of Ca content of coral skeleton by analyte additive method using the LIBS technique. *Opt. Laser Technol.* **44**(6): 1654-1659.

Haider, A. F. M. Y.., M. Rony, R. Lubna, and K. Abedin. 2011. Detection of multiple elements in coal samples from Bangladesh by laser-induced breakdown spectroscopy. *Opt. Laser Technol.* **43**(8): 1405-1410.

Haider, A. F. M. Y., M. Wahadoszamen, M. Sadat, K. M. Abedin, and A. Talukder. 2010. Elemental profiling and determination of Ti content of the beach sand samples of Bangladesh using LIBS technique. *Opt. Laser Technol.* **42**(6): 969-974.

Haider, A. F. M. Y., R. S. Lubna, and K. M. Abedin. 2012. Elemental analyses and determination of lead content in kohl (stone) by laser-induced breakdown spectroscopy. *Appl. Spectrosc.* **66**(4): 420-425.

Haque, N., A. Hughes, S. Lim, and C. Vernon. 2014. Rare earth elements: Overview of mining, mineralogy, uses, sustainability and environmental impact. *Resources* **3**(4): 614-635.

Krishnan, R., and M. Asundi. 1981. Zirconium alloys in nuclear technology. *P. Natl. A Sci. India C: Eng. Sci.* **4**(1): 41-56.

McMillan, N. J., R. S. Harmon, F. C. De Lucia, and A. M. Miziolek. 2007. Laser-induced breakdown spectroscopy analysis of minerals: carbonates and silicates. *Spectrochim. Acta Part B: At. Spectrosc.* **62**(12): 1528-1536.

McMillan, N. J., C. E. McManus, R. S. Harmon, F. C. De Lucia, and A. W. Miziolek. 2006. Laser-induced breakdown spectroscopy

analysis of complex silicate mineralsberyl. *Anal. Bioanal. Chem.* **385**(2): 263-271.

Miziolek, A. W.,V. Palleschi, and I. Schechter. 2006. Laser-Induced Breakdown Spectroscopy (LIBS): Fundamentals and Applications. U. K.: Cambridge University Press.

Peters, M., C. Leyens, U. Schulz, and W. A. Kaysser. 2001. EB-PVD thermal barrier coatings for aeroengines and gas turbines. *Adv. Eng. Mater.* **3**(4): 193-204.

Schulz, K. J., J. H. DeYoung, R. R. Seal, and D. C. Bradley. 2018. Critical Mineral Resources of the United States: Economic and Environmental Geology and Prospects for Future Supply: Geological Survey Professional Paper 1802, p. V1–V26, https://doi.org/10.3133/pp1802V.

Singh, J. P., and S. N. Thakur. 2006. Laser-Induced Breakdown Spectroscopy. U. K.: Elsevier.

Tasneem, F., Z. H. Khan, A. Islam, N. Faiza, S. M. Kabir, A. I. Talukder, A. F. M. Y. Haider, and M. Wahadoszamen. 2019. A Rapid Method of Identification of Garnet in Beach Sands Using Laser-Induced Breakdown Spectroscopy. *J. Bangladesh Acad. Sci.* **43**(2): 149-157.

Yun, J.-I., T. Bundschuh, V. Neck, and J.-I. Kim. 2001. Selective determination of europium (III) oxide and hydroxide colloids in aqueous solution by laser-induced breakdown spectroscopy. *Appl. Spectrosc.* **55**(3): 273-278.

*(Received 28 June 2020; accepted July 6, 2020)*